

## Enhanced Mobility of Organic Field-Effect Transistors with Epitaxially Grown C<sub>60</sub> Film by *in-situ* Heat Treatment of the Organic Dielectric

Th. B. Singh,<sup>1,§</sup> N. Marjanović,<sup>1</sup> G. J. Matt,<sup>1</sup> S. Günes,<sup>1</sup> N. S. Sariciftci,<sup>1</sup> A. Montaigne Ramil,<sup>2</sup> A. Andreev,<sup>2,†</sup> H. Sitter,<sup>2</sup> R. Schwödauer<sup>3</sup> and S. Bauer<sup>3</sup>

<sup>1</sup>Linz Institute for Organic Solar Cells (LIOS),

Physical Chemistry, Johannes Kepler University Linz, Austria

<sup>2</sup>Institute of Semiconductor- and Solid State Physics, Johannes Kepler University Linz, Austria

<sup>3</sup>Soft Matter Physics, Johannes Kepler University Linz, Austria

<sup>§</sup>Corresponding author. e-mail: birendra.singh@jku.at

### ABSTRACT

Electron mobilities were studied as a function of thin-film growth conditions in hot wall epitaxially grown C<sub>60</sub> based field-effect transistors. Mobilities in the range of ~ 0.5 to 6 cm<sup>2</sup>/Vs are obtained depending on the thin-film morphology arising from the initial growth conditions. Moreover, the field-effect transistor current is determined by the morphology of the film at the interface with the dielectric, while the upper layers are less relevant to the transport. At high electric fields, a non-linear transport has been observed. This effect is assigned to be either because of the dominance of the contact resistance over the channel resistance or because of the gradual move of the Fermi level towards the band edge as more and more empty traps are filled due to charge injection.

### INTRODUCTION

Research in Organic Field-Effect Transistors (OFETs) resulted in very interesting devices such as displays [1-3], all organic integrated circuits [4], gas sensors [5], identification tags [6-8], light sensors [9] and memory elements [10]. The measured charge carrier mobilities are 15 cm<sup>2</sup>/Vs for rubrene single crystal [11] and in excess of 1-2 cm<sup>2</sup>/Vs in the case of vacuum evaporated pentacene thin-films [12]. On the other hand, effort to increase charge carrier mobility in OFETs with n-type organic materials have been difficult due to several physical reasons: rapid degradation under ambient condition and electron transport properties are sensitive to purity of the crystal [13]. Among the n-type organic semiconductors, to mention a few, C<sub>60</sub> [14], methanofullerenes [15], fluorinated phthalocyanines [16], naphthalenes and N-substituted naphthalene 1,4,5,8-tetracarboxylic diimide [17] or N,N'-dialkyl-3,4,9,10-perylene tetracarboxylic diimide (PTCDI, PTCDI-C<sub>5</sub> [18] and PTCDI-C<sub>8</sub>H, correspondingly) show highest obtained mobilities of up to 0.6 cm<sup>2</sup>V<sup>-1</sup>s<sup>-1</sup> [19]. Most of these devices are grown on untreated inorganic SiO<sub>2</sub> or Al<sub>2</sub>O<sub>3</sub> dielectrics. Because of the very different physical nature of the two media, the deposition may result in highly disordered films, leading to a poor performance [20]. Although the van der Waals type interactions between organic molecules and inorganic substrates are rather weak, the crystallographic phases, the orientation, and the morphology of the resulting organic semiconductor films critically depends on the interface and growth kinetics. In field-effect devices, the first few monolayers closer to the dielectric determine the charge transport in organic semiconductor layers [21]. We have considered such interface related phenomena with an attempt by growing organic semiconductor layers on top of an organic

insulator and by studying their structure-performance relationships. In this paper, we present results on OFETs fabricated using hot wall epitaxially (HWE) grown  $C_{60}$  films on top of organic dielectrics. A good interfacial organisation of the resulting  $C_{60}$  film can be obtained by *in-situ* pre-heating the dielectric and depositing the organic semiconductor at a lower rate. The resulting OFETs exhibit mobilities in the range between 0.5 to 6  $\text{cm}^2/\text{Vs}$ .

## EXPERIMENTAL DETAILS

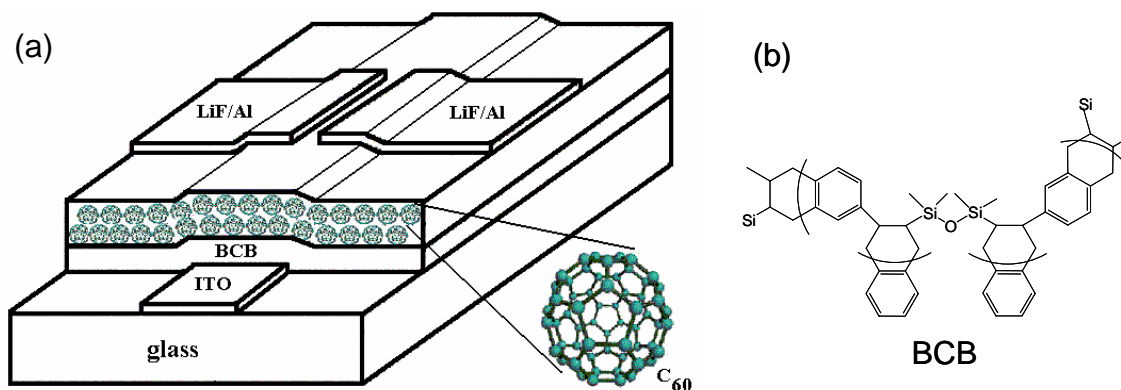


Figure 1: (a) Schematic of the top contact  $C_{60}$  OFET device structure, (b) Chemical Structure of BCB

In this study, we have chosen divinyltetramethyldisiloxane-bis(benzocyclobutane) (BCB, also known as “Cyclotene<sup>TM</sup>” from Dow Chemicals) as dielectric. Previous studies showed that BCB is a promising dielectric material possessing a large dielectric breakdown voltage, a nearly temperature independent thermal expansion coefficient and rather high glass transition temperature in excess of 350  $^{\circ}\text{C}$  [22,23]. A scheme of the device geometry and the molecular structure of the dielectric is shown in Figure 1. The device is fabricated on ITO/glass substrates. BCB (used as received from Dow chemicals) was spin coated at 1500 rpm for 1 minute from a 30 % molar solution in mesitylene yielding films with a thickness of  $\sim 1.7 \mu\text{m}$ . The first round of curing of the BCB was done by thermally cross-linking the polymer for 30 minutes at 250 $^{\circ}\text{C}$  in an Ar atmosphere. After cross-linking the BCB, the film is insoluble and practically free of residual organic solvents. In the second round, the BCB dielectric is pre-heated *in-situ* inside the hot wall epitaxy system under high vacuum conditions for 20 minutes (which means thermal surface cleaning before growth). All  $C_{60}$  films (thickness 5 nm and 300 nm) were grown by HWE on top of the dielectric at a constant substrate temperature of 130 $^{\circ}\text{C}$  at a deposition rate of 0.8  $\text{\AA}/\text{second}$ . Device transportation from the HWE system to the glove box for metal evaporation and further electrical characterisation was carried out under an argon environment. The top source and drain electrodes, (LiF/Al 0.6/60 nm) were evaporated under vacuum ( $2 \times 10^{-6}$  mbar) through a shadow mask. Other metals such as Au, Cr/Au, Ca/Al and Mg/Al were also evaporated for comparative studies. The channel length  $L$  of the device is 20-25  $\mu\text{m}$  and the channel width is  $W = 1.4 \text{ mm}$ , giving a  $W/L$  ratio of 200-300. For dielectric constant and capacitance-voltage measurements, separate devices with Metal-Insulator-Semiconductor (MIS) structures were fabricated under identical conditions and measured. From the measurement of the BCB film thickness,  $d \approx 1.7 \mu\text{m}$  and the dielectric constant of BCB,  $\epsilon_{BCB} \approx 2.6$ , a dielectric capacitance  $C_{BCB} \approx 1.3 \text{ nF}/\text{cm}^2$  was calculated. The electrical characterization of the devices was

carried out in an argon environment inside a glove box. An Agilent E5273A instrument was employed for the steady state current-voltage measurements. All measurements were performed with an integration time of 2 seconds in steps of 2 V. The surface morphology and the thickness of the dielectric and  $C_{60}$  films were measured in air with a Digital Instrument Dimension 3100 atomic force microscope.

### THIN-FILM MORPHOLOGY

At the first, topography images were taken with atomic force microscopy on bare dielectric surfaces resulting in a surface roughness below  $<5\text{nm}$  [15]. Hot wall epitaxially grown organic thin-films including  $C_{60}$  are expected to be highly ordered [24-25]. The morphologies of two 5 nm thick  $C_{60}$  films are shown in Figures 2(a)-2(b), demonstrating a striking difference of the morphology, if the growth proceeds on *in-situ* preheated substrates. The initial film growth kinetics seems to be different on *in-situ* preheated and non-treated substrates. One can see that on preheated dielectric at  $250\text{ }^{\circ}\text{C}$ , the resulting  $C_{60}$  film shows rather nanocrystalline-like structure, while amorphous-like  $C_{60}$  films are found on top of non treated substrates. In contrast, thicker  $C_{60}$  films (100 to 300 nm) show practically the same morphology as demonstrated in Figure 2(c)-2(d).

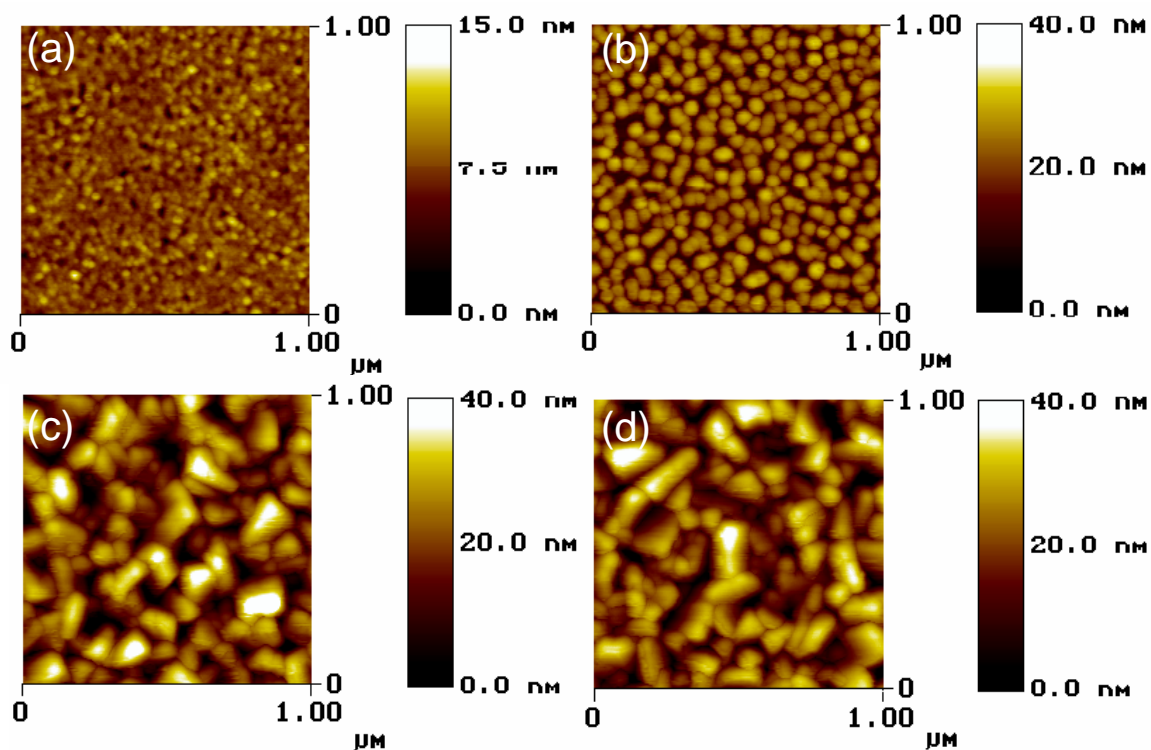


Figure 2: AFM topography images of (a) 5 nm  $C_{60}$  film grown on BCB substrates without pre-heating (b) 5 nm  $C_{60}$  film grown on BCB substrates with *in-situ* pre-heating at  $250\text{ }^{\circ}\text{C}$  (c) 300 nm of  $C_{60}$  film grown on top of BCB without pre-heating and (d) 300 nm of  $C_{60}$  film grown on top of BCB with *in-situ* pre-heating at  $250\text{ }^{\circ}\text{C}$ .

On *in-situ* preheated dielectric, interaction of  $C_{60}$  with BCB is reduced resulting in large crystalline structure of  $C_{60}$ . As the film thickness becomes higher, surface does not influence the growing which leads to the same morphologies irrespective of the initial growth condition.

## CURRENT-VOLTAGE CHARACTERISTICS

First we consider the transistor characteristics of  $C_{60}$  OFETs fabricated on non pre-heated dielectric surfaces. Figure 3(a) shows an n-channel OFET with a clear saturation of the drain-source current,  $I_{ds}$  for drain-source voltages,  $V_{ds}$  exceeding the applied positive gate voltage,  $V_{gs}$ .  $I_{ds}$  in the range of sub-mA are routinely obtained in these devices. The transfer characteristic ( $I_{ds}(V_{gs})$ ) in the saturated region with a  $V_{ds}=60$  V features a negligible hysteresis as shown in Figure 3(b).  $I_{ds}$  increases quadratically with  $V_{gs}$  which we fit to the well known equation (1) [26]:

$$I_{ds} = \frac{\mu WC_{BCB}}{2L} (V_{gs} - V_t)^2 \quad (1)$$

where  $V_t$  is the onset voltage. We observed only a slight deviation (see especially the  $\sqrt{I_{ds}(V_{gs})}$  plot in Figure. 3(b)) from the theoretical fit to the experimental data which indicates a nearly  $V_{gs}$  independent mobility,  $\mu_e$ .

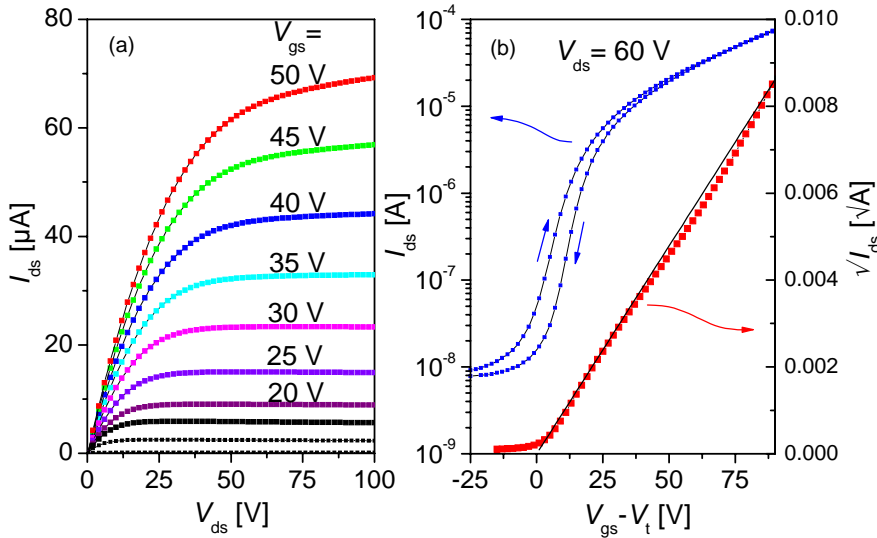


Figure 3: (a) Output Characteristics ( $I_{ds}(V_{ds})$ ) of  $C_{60}$  FETs based on without preheated dielectric BCB (b) Transfer Characteristics ( $I_{ds}(V_{gs})$ ) of  $C_{60}$  FETs based on without preheated dielectric BCB,  $\sqrt{I_{ds}(V_{gs})}$  plots on the right scale for the data taken from the descending curve along with a theoretical fit using equation (1).

Second, we will now consider OFETs fabricated with  $C_{60}$  films grown on *in-situ* preheated substrates at  $250$  °C. These OFETs are found to have a high intrinsic conductivity (see Figure 4). Figure 4(a) shows an n-channel transistor with its saturated regime  $I_{ds}$  having a  $V_{gs}$  independent slope which is the signature of high intrinsic conductivity. Origin of such an observation is the increased mobility and not doping. Doping can be excluded as the  $C_{60}$  film was grown in a clean HWE set up in addition to cleaning of BCB dielectric layer due to pre-

heating. In the OFETs fabricated on *in-situ* preheated substrates we observed for the same  $V_{gs}$  an increase in  $I_{ds}$  at least by 3 times, as compared to those on non-preheated substrates. Further all the curves are replotted by subtracting the bulk current  $I_{ds}(V_{ds})$  for  $V_{gs} = 0$  V from the respective curves (represented by dashed curves). In the corrected curves (dash curves) we observed a well defined pinch-off  $I_{ds}(V_{ds})$  for an applied  $V_{gs}$ . Applying a large  $V_{gs}$  resulted in a non-linear  $I_{ds}(V_{ds})$  curve as shown in Figure 4(b). This observation can be due to a voltage dependency of the mobility. In [27,28] such non-linearities are theoretically outlined. Therein  $\mu(V_{gs})$  is attributed due to trap-filling effects and/or space-charge limited currents of the drain current itself beside the gate induced space charge. However at low  $V_{gs}$  space charge limited current and trap-filling are negligible and not observable in the output characteristics. Although in [29-31], it has been mentioned that LiF/Al is ohmic contact of  $C_{60}$ , since we observed a weak deviation from linearity of  $I_{ds}(V_{ds})$  at low  $V_{ds}$ , there exists a low contact resistance [32]. A very similar phenomena happens in the case of reduced channel lengths [33]. However in the present studies, for calculating  $\mu_e$ , the contact resistance is not taken into account. On the other hand it can also be mentioned that such a large magnitude of the current density is observed only in semiconductors with low trap densities. These traps can be filled with large carrier injection/accumulation. This phenomena leads to a trap filled regime, a behaviour which is normally observed very rarely [34, 35].

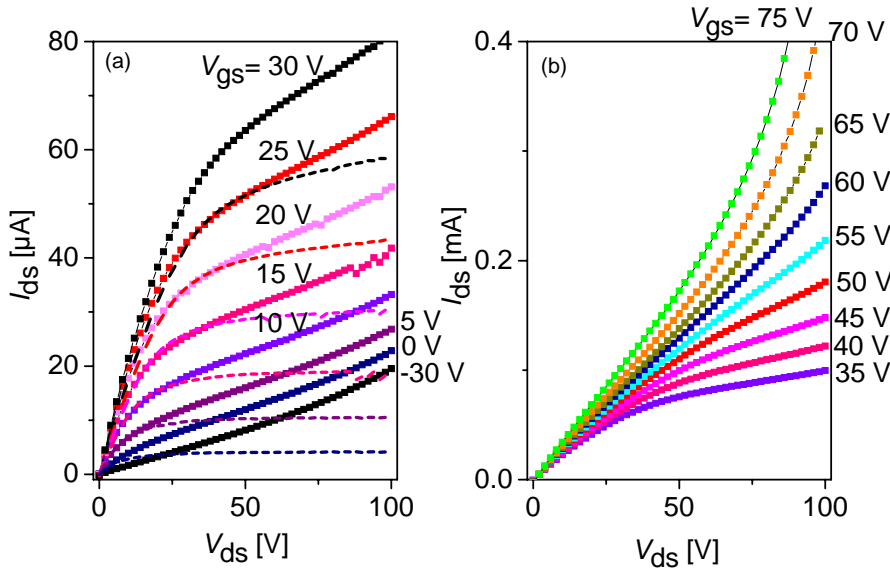


Figure 4: Output Characteristics of  $C_{60}$  OFETs on *in-situ* pre-heated dielectric BCB at 250 °C. (a)  $I_{ds}(V_{ds})$  curves (symbols) where the bulk current has been subtracted from all the respective curves (dash curves) (b)  $I_{ds}(V_{ds})$  curves at high applied  $V_{gs}$ .

Finally we compared the transfer characteristics of all the OFETs fabricated under different film growth conditions. As shown in the plot of  $\sqrt{I_{ds}(V_{gs})}$ , (Figure 5), the slope,  $\Delta\sqrt{I_{ds}}/\Delta V_{gs}$  for the OFETs with *in-situ* pre-heated dielectric at 300 °C is much higher than the one with a non treated dielectric. In Figure 5 original data points are taken without subtracting the bulk current. Theoretical fits curves (without symbols) of the experimental data using equation (1) are also plotted in Figure 5. The theoretical curves agree reasonably well with the experimental curves suggesting a constant  $\mu_e$  as function of  $V_{gs}$  in the range of voltages

investigated. Accordingly,  $\mu_e$  calculated using equation (1) increased from 0.5 - 6  $\text{cm}^2/\text{Vs}$  as a results of *in-situ* pre-heating the dielectric layer. Previous reports on  $\text{C}_{60}$  FETs grown on  $\text{SiO}_2$  have shown a highest obtained  $\mu_e$  of 0.5  $\text{cm}^2/\text{Vs}$  [14]. The increase in  $\mu_e$  could be attributed due to the transition (while going from the unheated to the *in-situ* pre-heated dielectric) from disordered interface made of dendritic grains of different orientations with a rather high concentration of defects, mainly located at grain boundaries, to a well ordered  $\text{C}_{60}$  film as depicted in Figure 2(a)-2(b). Further analysis shows a  $V_{\text{gs}}$  independent  $\mu_e$  as a function of ordering. These observations go beyond the scope the present paper.

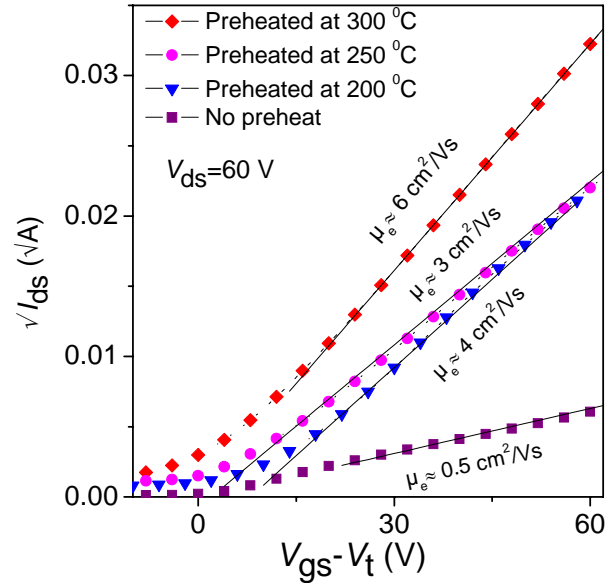


Figure 5:  $\sqrt{I_{\text{ds}}}$  versus  $V_{\text{gs}}$  plots (symbols) for  $\text{C}_{60}$  OFETs fabricated with different growth conditions along with theoretical fit curves (without symbols) using equation (1). The obtained electron mobilities,  $\mu_e$  are indicated along with the respective curves.

## DISCUSSION

As discussed in detail by Horowitz et al [36], for FET with high mobility, mobility is not dependent on gate voltage as observed in the present study. The contact resistance becomes more important for extracting parameters from the current-voltage curves. We have used other contacts such as Au, Cr/Au, Mg/Al and Ca/Al. Among all these contacts, better current injection is obtained with LiF/Al. Hence the argument of a better electron injection with a lower work function electrode does not hold in the present study. Previous studies have shown pinning of Fermi-level at the interface of metal- $\text{C}_{60}$ . LiF is proposed to be lowering the barrier for electron injection from the studies of organic solar cells [29-31]. The observation of a structure-performance relationship seems to be notable. However X-ray diffraction studies did not reveal any significant changes on the crystallographic phases of the  $\text{C}_{60}$  films grown on dielectrics with and without pre-heating. This might be caused by the fact that x-rays probe bulk properties of the semiconductor films. The most important parameter is the morphologies of the first few monolayer of  $\text{C}_{60}$  (Figure 2). Films with large crystal features a high current and it is proposed that these films has a lower trap density resulting high non-linear transport phenomena (Figure 4) as a result of trap filling effect at large gate voltage. Detailed studies are required in order to

understand the complete growth kinetics of the semiconducting  $C_{60}$  films in these devices. Post-production treatment may also bring new effects in the devices.

## CONCLUSIONS

In conclusion, we have demonstrated n-channel OFETs with an electron mobility of 0.5-6  $\text{cm}^2\text{V}^{-1}\text{s}^{-1}$ . The obtained mobility is found to be strongly dependent on the film morphology which in turn strongly depends on an in-situ treatment of the gate dielectric prior to the semiconductor film growth. At high applied gate voltages, a non-linear transport is observed either due to trap-filling effects or contact resistance dominating over the channel resistance.

## ACKNOWLEDGEMENT

The authors gratefully acknowledges fruitful discussions with Gilles Horowitz from Institute de Interfaces, Traitements, Organisation et Dynamique des Systèmes (ITODYS) CNRS, France. Special thanks are to Michael Auinger and Philipp Stadler for technical help. Financial support from the Austrian Foundation for the Advancement of Scientific Research (FWF P15155, P15627 and P15629) and FWF NANORAC contract No. N00103000 are acknowledged.

†Present address: Institute for Physics, University Leoben, Franz-Josef-Str. 18, A-8700 Leoben, Austria.

## REFERENCES

1. J. A. Rogers, Z. Bao, K. Baldwin, A. Dodabalapur, Brian Crone, V. R. Raju, V. Kuck, H. Katz, K. Amundson, J. Ewing, and P. Drzaic, *Proc. Natl. Acad. Sci.* **98**, 4835 (2001).
2. H. E. A. Huitema, G. H. Gelinck, J. B. P. H. van der Putten, K. E. Kuijk, C. M. Hart, E. Cantatore, P. T. Herwig, A. J. J. M. van Breemen and D. M. de Leeuw, *Nature* **414**, 599 (2001).
3. C. D. Sheraw, L. Zhou, J. R. Huang, D. J. Gundlach, T. N. Jackson, M. G. Kane, I. G. Hill, M. S. Hammond, J. Campi, B. K. Greening, J. Francl and J. West, *Appl. Phys. Lett.* **80**, 1088 (2002).
4. A. R. Brown, C. P. Jarret, D. M. de Leeuw, M. Matters, *Synth. Met.* **88**, 37 (1997).
5. B. K. Crone, A. Dodabalapur, R. Sarpeshkar, A. Gelperin, H. E. Katz, and Z. Bao, *J. Appl. Phys.* **91**, 10140 (2001).
6. D. M. De Leew, G. H. Gelinck, T. C. T. Geuns, E. Van Veenendaal, E. Cantatore and B. H. Huisman, *Int. Electron Device Meeting (IEDM) Tech. Dig.* 293 (2002).
7. P. F. Baude, D. A. Ender, M. A. Haase, T. W. Kelley, D. V. Muyres, and S. D. Theiss, *Appl. Phys. Lett.* **82**, 3964 (2003).
8. H. Klauk, M. Halik, U. Zschieschang, F. Eder, G. Schmid, and Ch. Dehm, *Appl. Phys. Lett.* **82**, 4175 (2003).
9. K. S. Narayan and N. Kumar, *Appl. Phys. Lett.* **79**, 1891 (2001).

10. R. Schroeder, L. A. Majewski and M. Grell, *Adv. Mater.* **16**, 633 (2004); Th. B. Singh, N. Marjanović, G. J. Matt, N. S. Sariciftci, R. Schwödiauer and S. Bauer, *Appl. Phys. Lett.* **85**, 5409 (2004).
11. V. C. Sundar, J. Zaumseil, V. Podzorov, E. Menard, R. L. Willett, T. Someya, M. E. Gershenson and J. A. Rogers, *Science* **303**, 1644 (2004).
12. Y. -Y. Lin, D. J. Gundlach, S. F. Nelson and T. N. Jackson, *IEEE Electron Devices Lett.* **18**, 606 (1997).
13. R. G. Kepler, *Phys. Rev.* **119**, 1226 (1960).
14. S. Kobayashi, T. Takenobu, S. Mori, A. Fujiwara, and Y. Iwasa, *Appl. Phys. Lett.* **82**, 4581 (2003).
15. Th. B. Singh, N. Marjanović, P. Stadler, M. Auinger, G. J. Matt, S. Günes, N. S. Sariciftci, R. Schwödiauer and S. Bauer, *J. Appl. Phys.* (in press)
16. Z. Bao, A. J. Lovinger and J. Brown, *J. Am. Chem. Soc.* **120**, 207 (1998).
17. H. E. Katz, J. Johnson, A. J. Lovinger and W. Li, *J. Am. Chem. Soc.* **122**, 7787 (2000).
18. R. J. Chesterfield, J. C. McKeen, Ch. R. Newman, C. D. Frisbie, P. C. Ewbank, K. R. Mann and L. L. Miller, *J. Appl. Phys.* **95**, 6396 (2004).
19. P. R. L. Malenfant, C. D. Dimitrakopoulos, J. D. Gelorme, L. L. Kosbar and T. O. Graham, *Appl. Phys. Lett.* **80**, 2517 (2002).
20. G. Horowitz, Ph. Lang, M. Mottaghi, and H. Aubin, *Adv. Funct. Mater.* **14**, 1069 (2004).
21. F. Dinelli, M. Murgia, P. Levy, M. Cavallini, F. Biscarini and D. M. de Leeuw, *Phys. Rev. Lett.* **92**, 116802 (2004).
22. R. Schwödiauer, G. S. Neugschwandtner, S. Bauer-Gogonea, S. Bauer and W. Wirges, *Appl. Phys. Lett.* **75**, 3998 (1999).
23. [www.dow.com/cyclotene/](http://www.dow.com/cyclotene/)
24. A. Andreev, G. Matt, C. J. Brabec, H. Sitter, D. Badt, H. Seyringer and N. S. Sariciftci *Adv. Mat.* **12**, 629 (2000).
25. D. Stifter and H. Sitter, *Appl. Phys. Lett.* **66**, 679 (1995).
26. S. M. Sze, *Physics of Semiconductor Devices* (Wiley, New York, 1981).
27. G. Horowitz and P. Delannoy, *J. Appl. Phys.* **70**, 469 (1991).
28. M. Koehler and I. Biaggio, *Phys. Rev. B.*, **70**, 045314 (2004).
29. V. D. Mihailetschi, J. K. J. van Duren, P. W. M. Blom, J. C. Hummelen, R. A. J. Janssen, J. M. Kroon, M. T. Rispens, W. J. H. Verhees and M. M. Wienk, *Adv. Funct. Mater.* **13**, 43 (2003);
30. G. J. Matt, N. S. Sariciftci and T. Fromherz, *Appl. Phys. Lett.* **84**, 1570 (2004).
31. C. J. Brabec, A. Cravino, D. Meissner, N. S. Sariciftci, T. Fromherz, M. T. Rispens, L. Sanchez and J. C. Hummelen, *Adv. Funct. Mater.* **11**, 374 (2001).
32. G. Horowitz, private communications.
33. E. J. Meijer, G. H. Gelinck, E. Van Veenendaal, B. H. Huisman, D. M. De Leeuw, T. M. Klapwijk, *Appl. Phys. Lett.*, **82**, 4576 (2003).
34. A. Rose, *Phys. Rev.* **97**, 1538 (1955).
35. M. A. Lampart, *Phys. Rev.* **103**, 1648 (1956).
36. W. Kalb, Ph. Lang, M. Mottaghi, H. Aubin, G. Horowitz and M. Wutting, *Synth. Met.*, **146**, 279 (2004).